is unexplained. Further investigations of the sign of the charge carriers at different temperatures should be carried out.

In order to avoid the effect of space charge, the frequency of the applied electric field was varied from 30 cps to 700 cps. Hall mobilities obtained at various frequencies are shown in Fig. 2. We obtained about 2 cm²/volt sec as Hall mobility of a hole from the higher frequency values. Such a small mobility seems to be

reasonable in ionic crystals, but seems to be too small to interpret Day's experiments. We know, in Fig. 4 of his paper,[3] that the holes produced by light in the β band have a "Schubweg" of about 10^{-2} cm under the applied field of 3.8×10^3 volt/cm. By using hole mobility of 2 cm²/volt sec, the lifetime of holes is calculated to be about 10^{-6} second. This lifetime seems to be too large, because there are so many defects in the neutron-irradiated specimens to shorten the lifetime.

Infrared Absorption in n-Type Germanium*

H. Y. Fan, W. Spitzer, and R. J. Collins†
Purdue University, Lafayette, Indiana
(Received August 22, 1955)

Theory of absorption by free carriers is given taking into account the effects of scattering by impurities and by lattice vibrations. Experimental results are reported for n-type germanium samples of various carrier and impurity concentrations. The measurements were made in the temperature range between 78°K and 450°K, covering a wavelength region from 5 to 38 microns. At the high-temperature end, the absorption is proportional to the carrier concentration, lattice scattering being the dominant effect. At 78°K, the absorption per unit carrier concentration consists of a constant part and a part proportional to the impurity concentration. The absorption increases with wavelength more rapidly at the low temperature. The frequency and temperature dependences of absorption in the various samples are in good agreement with the theory. Quantitative agreement can be obtained by using an effective mass $m^* \approx 0.1m$.

INTRODUCTION

ABSORPTION of light in germanium falls sharply when the photon energy becomes smaller than the energy gap of the material, which corresponds to about 1.8 microns at room temperature. The relatively weak absorption at longer wavelengths varies with the conductivity of the specimen and seems to depend on the concentration of the conduction carriers.[1] In p-type germanium, the spectral absorption curve shows band structures,[2] and it has been shown that the absorption is associated with electron transitions between overlapping energy bands in the valence band.[3] In n-type germanium, however, the absorption increases smoothly with increasing wavelength.[1,2,4] It seems that, instead of interband transitions, the absorption is a free electron effect, i.e., in the absorption process the excited electron remains in the same energy band. Free electrons do not give absorption because of the difficulty of satisfying both the conservation of energy and the conservation of momentum. These conditions

can be fulfilled through the electron interaction with the crystal lattice. The absorption depends on the electron-lattice collision frequency, which also determines the conduction properties of the crystal.

In the following, we shall first discuss the theory of absorption which was only briefly outlined in a previous publication.[1] Experimental results obtained over a wide wavelength region on different samples and at different temperatures will then be presented. The results will be correlated with the electrical properties of the samples and compared with the theory.

THEORY

The absorption coefficient is related to the conductivity by

$$\alpha = 4\pi\sigma/cn, \tag{1}$$

where n is the refractive index. The relationship between the conductivity and the absorption probability for a photon, P_a, is

$$\sigma = (\epsilon/4\pi)P_a, \tag{2}$$

ϵ being the dielectric constant. Theoretically, either P_a or directly σ is calculated.

The effect of conduction electrons in crystals was treated quantum mechanically by Kronig.[5] However, the electron-lattice interaction was taken into account in the same way as in the classical theory of Drude, by

* Work supported by U. S. Signal Corps Contract.
† Now at Bell Telephone Laboratories, Murray Hill, New Jersey.
[1] H. Y. Fan and M. Becker, *Proceedings of the Reading Conference* (Butterworths Scientific Publications, London, 1951), pp. 132–147.
[2] Kaiser, Collins, and Fan, Phys. Rev. **91**, 1380 (1953); H. B. Briggs and R. C. Fletcher, Phys. Rev. **87**, 1130 (1952) and Phys. Rev. **91**, 1342 (1953).
[3] A. H. Kahn, Phys. Rev. **97**, 1647 (1955).
[4] Spitzer, Collins, and Fan, Phys. Rev. **98**, 1536 (1955).

[5] R. de L. Kronig, Proc. Roy. Soc. (London) A133, 245 (1931).

introducing a damping factor corresponding to a broadening of the resonance frequency $\omega_0=0$ of free electrons. The expression obtained for the conductivity is the same as in the classical theory:

$$\sigma = \frac{n_e e^2}{m^*}\frac{1/\tau}{\omega^2+(1/\tau)^2},\qquad(3)$$

where n_e is the electron concentration and $1/\tau$ is the electron-lattice collision frequency. Only the effective mass m^* appears instead of the free electron mass. The factor $(1/\tau)$ is estimated from dc conductivity by putting $\omega=0$. Usually $(1/\tau)$ is much smaller than ω in the infrared region:

$$\sigma = \frac{n_e e^2}{m^*}\frac{1}{\tau\omega^2}=\sigma_0\frac{1}{\tau^2\omega^2}.\qquad(4)$$

The introduction of a constant damping factor for different transition processes of all electrons cannot be a satisfactory approximation. If $\hbar\omega$ is much smaller than the thermal energy of the electrons, the electron-lattice collision frequency can be taken as a function of the initial electron energy only, and we can average $(1/\tau)/[\omega^2+(1/\tau)^2]$ over the equilibrium distribution of electron energy. With this improvement, the expression should give good results at low frequencies. However, $\hbar\omega$ in the infrared region is comparable or larger than the average electron energy, kT, in semiconductors. It is therefore necessary to treat more properly the electron-lattice interaction. The interaction arises from disturbances in the periodic potential field of the crystal due to lattice vibrations and impurities or defects in the lattice.

Lattice Vibration

The effect of lattice vibration can be treated by the second-order time dependent perturbation method.[6] Photon absorption is accompanied by the absorption or emission of a phonon. The probability of an absorption process is given by the usual expression

$$P = \frac{2\pi}{\hbar}\sum_i \frac{|H_{0i}H_{if}|^2}{(E_i-E_0)^2}\rho,\qquad(5)$$

where subscripts $0, i, f$ refer to the initial, intermediate, and final states, respectively. ρ is the number of final states per unit energy range. Of the two matrix elements of perturbation, H_{0i} and H_{if}, one is for the radiation field and the other is for the lattice vibration. To get the absorption probability for a photon, the radiation field will be normalized for one photon in the crystal. Consider the electrons as free in the unperturbed state, with an effective mass m^*. For the perturbation by the radiation field, the matrix element connecting two states is not zero, only when the two states have

[6] This treatment is due to H. Fröhlich as pointed out in reference 1.

approximately the same wave-number vector $\mathbf{k}$ for the electron.

$$H^{(\nu)}=-\frac{1}{(V\epsilon)^{\frac{1}{2}}}\frac{e\hbar^2}{m^*}\left(\frac{2\pi}{\hbar\omega}\right)^{\frac{1}{2}}k\cos(\mathbf{p}_\nu,\mathbf{k}),\qquad(6)$$

where V is the volume of the crystal and $\mathbf{p}_\nu$ is the direction of polarization. The perturbation by the lattice vibration has nonvanishing matrix elements only for two states differing in $\mathbf{k}$ by $\pm\mathbf{q}$.

$$H^{(l)}=\pm i\left(\frac{\Omega}{V}\right)^{\frac{1}{2}}\frac{2}{3}\left(\frac{\hbar}{2M\omega_q}\right)^{\frac{1}{2}}Cq\begin{cases}(n_q)^{\frac{1}{2}},\\(n_q+1)^{\frac{1}{2}},\end{cases}\qquad(7)$$

where Ω is the volume of a primitive cell, M is the reduced mass of atoms in a cell, and C is a parameter which may be taken as a constant. q, n_q, and ω_q are, respectively, the wave number, quantum number and frequency of the phonon. $(n_q)^{\frac{1}{2}}$ applies for phonon absorption and $(n_q+1)^{\frac{1}{2}}$ applies for phonon emission.

In an absorption process, the photon absorption may be either preceded or followed by the phonon interaction. With photon absorption first, we have

$$\mathbf{k}_i=\mathbf{k}_0,\quad \mathbf{k}_f=\mathbf{k}_0\mp\mathbf{q},$$
$$E_i-E_0=-\hbar\omega.\qquad(8)$$

With phonon interaction first, we have

$$\mathbf{k}_i=\mathbf{k}_f,\quad \mathbf{k}_i=\mathbf{k}_0\mp\mathbf{q},$$
$$E_i-E_0=\frac{\hbar^2}{2m^*}(k_i{}^2-k_0{}^2)\pm\hbar\omega_q.\qquad(9)$$

The upper alternate sign in these expressions corresponds to phonon emission whereas the lower sign corresponds to phonon absorption. There are thus four different absorption processes.

The energy of the final state is

$$E_f=E_0+\frac{\hbar^2}{2m^*}(k_f{}^2-k_0{}^2)\pm\hbar\omega_q-\hbar\omega=E_0+\frac{\hbar^2}{2m^*}q^2$$
$$\mp 2k_0q\cos(\mathbf{k}_0,\mathbf{q})\pm\hbar\omega_q-\hbar\omega.\qquad(10)$$

Each final state corresponds to a definite $\mathbf{q}$. The number of $\mathbf{q}$'s in a volume $d\Omega_q$ in $\mathbf{q}$ space is $Vd\Omega_q/(2\pi)^3$, therefore the number of final states per unit energy range is

$$\rho=\frac{V}{(2\pi)^3}\frac{d\Omega_q}{dE_f}=\frac{V}{(2\pi)^3}\frac{q^2\sin\theta dqd\theta d\varphi}{dE_f}=\frac{V}{(2\pi)^3}\frac{m^*q}{\hbar^2k_0}dqd\varphi.\qquad(11)$$

The quantum number n_q in the matrix element of phonon interaction is given by

$$n_q=[\exp(\hbar\omega_q/kT)-1]^{-1}.\qquad(12)$$

The effect of optical modes is small in determining the carrier mobility but their effect on absorption is not necessarily small,[7] since the condition is not the same

[7] J. Bardeen, Phys. Rev. 79, 216 (1950).

as in the interaction with electrons of thermal energy. However, the following consideration shows that the effect of optical modes is unimportant. The energy of optical phonons is about 0.0421 ev or $k(489°K)$, as estimated from the frequency, 340 cm^{-1}, of the strongest lattice absorption band. It has also been estimated to be $k(520°K)$. Thus below 500°K, absorption with phonon absorption is small, since n_q is small. Furthermore, such a process will change with temperature much more rapidly than the observed absorption. On the other hand, absorption with phonon emission cannot take place if the sum of the photon energy and the thermal energy of the electron is less than the phonon energy. Thus, at 100°K, the effect of the optical phonons should become negligible at wavelengths >40 microns. Measurements made at long wavelengths do not show such behavior. On the basis of these considerations, we shall calculate only the effect of acoustical phonons. The phonon energy $\hbar\omega_q = \hbar s q$, s being the velocity of sound waves. The range of q is limited by the condition (10). It can be readily shown that $\hbar s q < kT$ for the conditions of our experiments, $T > 78°K$ and $\lambda > 5$ microns. We can therefore use the approximation $n_q = kT/\hbar\omega_q$ and neglect the factor 1 in $(n_q + 1)$.

The probability of absorption for a photon due to a single electron is obtained by adding the probabilities, P's, of the four types of processes and integrating over dq and $d\varphi$ in the expression (11) of ρ. The result is averaged over the electrons and multiplied by the number of electrons, giving the total absorption probability for a photon

$$P_a = \frac{16}{27} n_e \frac{\Omega e^2 C^2 (2m^*)^{\frac{1}{2}}}{\epsilon \hbar^2 M s^2} \frac{kT}{(\hbar\omega)^{\frac{3}{2}}}$$

$$\times \left\langle \left(1 + 2\frac{E_k}{\hbar\omega}\right)\left(1 + \frac{E_k}{\hbar\omega}\right)^{\frac{1}{2}} \right\rangle. \quad (13)$$

The product of the last two brackets is averaged over the equilibrium energy distribution of the electrons. The dc conductivity is given by

$$\sigma_{l0} = \frac{n_e e^2}{m^*}\tau = \frac{n_e e^2}{m^*}\frac{3\sqrt{\pi}}{\sqrt{2}}\frac{\hbar^4 M s^2}{(m^* kT)^{\frac{3}{2}} C^2 \Omega}, \quad (14)$$

when the scattering of electrons is determined by the lattice vibration. Introducing σ_{l0} in (13) and using the relation (2), we get a conductivity due to lattice interaction

$$\sigma_l = \frac{4}{9\sqrt{\pi}}\sigma_{l0}\frac{1}{\tau^2\omega^2}\left(\frac{\hbar\omega}{kT}\right)^{\frac{1}{2}}\left\langle \left(1 + 2\frac{E_k}{\hbar\omega}\right)\left(1 + \frac{E_k}{\hbar\omega}\right)^{\frac{1}{2}} \right\rangle. \quad (15)$$

This expression is to be compared with (3) of the semiclassical theory. For $\hbar\omega > kT$, the quantity to be averaged is approximately equal to one, and we get a $\omega^{-1.5}$ dependence instead of ω^{-2} relation given by the

older theory. Also the temperature dependence is given by $(\tau^2 T)$ instead of τ^2.

Impurities

Impurities and lattice defects acting as scattering centers for free electrons can give rise to absorption. The scattering is strong if the centers are electrically charged and we shall be interested mainly in the effect of ionized impurities. The scattering centers will therefore be treated approximately as fixed point charges in a medium with the dielectric constant of the crystal. The problem can be treated in the same way as for the previous case, using the second-order perturbation method. To evaluate the matrix elements for the perturbation Hamiltonian it is necessary to take into account the screening of the charged center by the conduction electrons though the result is not sensitive to the expression of the screening effect. For classical distribution of conduction electrons, we may use for the perturbing potential

$$V_p = \frac{Ze}{\epsilon r} \exp(-r/l_D), \quad (16)$$

where l_D is the characteristic length in the Debye-Hückel theory of electrolytes. Using plane waves for the electrons, we get the matrix element

$$H_{k_1 k_2}{}^{(I)} = \frac{4\pi e^2}{V}\frac{1}{\epsilon}\frac{1}{|\mathbf{k}_1 - \mathbf{k}_2|^2 + (1/l_D)^2}. \quad (17)$$

Since the photon absorption involves negligible change in the wave vector of the electron, we have $\mathbf{k}_1 = k_0$ and $\mathbf{k}_2 = k_f$. The energy conservation gives

$$\frac{\hbar^2}{2m^*}k_f{}^2 = \hbar\omega + \frac{\hbar^2}{2m^*}k_0{}^2 \approx \hbar\omega + kT. \quad (18)$$

Therefore

$$|\mathbf{k}_2 - \mathbf{k}_1|^2 \gtrsim (k_2 - k_1)^2 > \frac{1}{2}\frac{2m^*}{\hbar^2}\hbar\omega. \quad (19)$$

For $\hbar\omega > 0.02$ ev ($\lambda < 62$ microns), $|\mathbf{k}_2 - \mathbf{k}_1|^2 > 3 \times 10^{13}$ cm^{-2}. On the other hand,

$$(1/l_D)^2 = 4\pi e^2 n_e / \epsilon kT. \quad (20)$$

For $T > 80°K$ and $N < 10^{18}$ cm^{-3}, $(1/l_D)^2 < 1.6 \times 10^{13}$ cm^{-2}. We shall therefore neglect $(1/l_D)^2$ in (17). For the range of our experiments, this approximation should give small errors. Carrying through the calculations, we get

$$P_a = \frac{N_i n_e}{\epsilon}\frac{16\sqrt{2}\pi^2}{3}\left(\frac{Ze^2}{\epsilon}\right)^2\frac{e^2\hbar^2}{m^{*\frac{5}{2}}}\frac{1}{(\hbar\omega)^{3.5}}$$

$$\times \left\langle \left(1 + 2\frac{E_{k_0}}{\hbar\omega}\right)\left(1 + \frac{E_{k_0}}{\hbar\omega}\right)^{\frac{1}{2}} \right\rangle; \quad (21)$$

where N_i is the concentration of charged centers.

The absorption can also be calculated as first-order perturbation if the wave functions of the electrons in the field of the scattering center were obtained. The absorption is essentially the inverse process of bremsstrahlung which has been treated in this way by Sommerfeld using unscreened Coulomb potential.[8] The matrix element of the dipole moment, averaged over the directions of the electron wave vector relative to the radiation field, is given by

$$\langle M_{0f}^2\rangle_{Av} = \frac{e^2}{V}\frac{2}{3}(4\pi)^2\left(\frac{Ze^2}{\epsilon}\right)^2\left(\frac{\hbar^2}{2m^*}\right)^2$$

$$\times \frac{1}{(\hbar\omega)^4}\frac{1}{k_0 k_f}\ln\left(\frac{k_f+k_0}{k_f-k_0}\right). \quad (22)$$

The probability for a photon to be absorbed by a conduction electron of wave vector k_0 in the potential field of one scattering center can be readily calculated by using this expression. Multiplying by the number of scattering centers and integrating over the number of conduction electrons, we get

$$P_a = \frac{N_i n_e}{\epsilon}\frac{16\pi^2}{3}\left(\frac{Ze^2}{\epsilon}\right)^2\frac{e^2\hbar}{m^*}\frac{1}{(\hbar\omega)^3}\left\langle\frac{1}{k_0}\ln\left(\frac{k_f+k_0}{k_f-k_0}\right)\right\rangle, \quad (23)$$

in which the wave numbers of the electron before and after the absorption is related by

$$(\hbar^2/2m^*)k_f^2 = (\hbar^2/2m^*)k_0^2 + \hbar\omega.$$

For electron obeying classical distribution,

$$\left\langle\frac{1}{k_0}\ln\left(\frac{k_f+k_0}{k_f-k_0}\right)\right\rangle = 2\hbar(2\pi m^* kT)^{-\frac{1}{2}}$$

$$\times \exp(\hbar\omega/2kT)K_0(\hbar\omega/2kT), \quad (24)$$

where K_0 is the modified Bessel function of order zero. This result reduces to the previous expression (21) if $\hbar\omega$ is much larger than E_{k0}, the thermal energy of the electrons. The effect of charged scattering centers gives an absorption with stronger frequency dependence, approximately $\omega^{-3.5}$, as compared to the effect of lattice vibration. On the other hand, the absorption should be rather insensitive to the temperature.

Recently, the same result was obtained by Wolfe.[9] An expression was derived for screened Coulomb potential of the type (16), which is in the form of an integral which is difficult to evaluate. The result reduces to (23) if the screening is neglected.

EXPERIMENTAL

A number of specimens of different carrier concentrations were used. The transmission measurements were made in a wavelength region from 5 to 30 microns

[8] A. Sommerfeld, Ann. Physik **11**, 257 (1931).
[9] R. Wolfe, Proc. Phys. Soc. (London) **A67**, 74 (1954).

TABLE I. A list of samples used in the optical measurements. The first column gives the Hall coefficient (R, cm³/coulomb) at 294°K; the second column gives the resistivity (ρ, ohm cm) at 294°K; the third column gives the carrier concentrations (n_e, cm⁻³); the fourth column gives the impurity concentration (N_i, cm⁻³) for those samples used for optical measurements at low temperature (78°K).

Column No. Sample No.	1 $R_{294 K}$	2 $\rho_{294 K}$	3 $n_e(10^{17})$	4 $N_i(10^{17})$
1	4.8	0.0045	15.9	25.2
2	6.2	0.0057	12.3	
3	7.5	0.0061	9.8	
4	9.3	0.0063	7.5	10.5
5	15.(0)	0.010	4.7	8.94
6	23.(0)	0.022	3.4	20.4
7	25.(2)	0.015	2.7	4.91
8	39.(6)	0.022	1.60	2.44
9	53.(7)	0.026	1.21	
10	140	0.050	0.47	0.578
11	156	0.065	0.41	0.685
12	83	0.06	0.84	11.05

using a double-pass Perkin Elmer monochromator. The samples used were single crystals with polished surfaces. Complete measurements were made at three temperatures: 450°K, 293°K, and 78°K.

Table I presents a list of the samples used with the data obtained from electrical measurements. The room temperature carrier concentrations, n_e, in column 3 were determined from the measured values of resistivity and Hall coefficient using the method of Johnson and Lark-Horovitz.[10] In the determination of n_e, the room temperature lattice scattering mobility was assumed to be 3800 cm² volt⁻¹ sec⁻¹. In each sample, the concentration is the same at the three temperatures. At 450°K, the intrinsic electron concentration (7×10^{15} cm⁻³) is considerably smaller than the lowest value of n_e at room temperature as given in Table I. At 78°K,
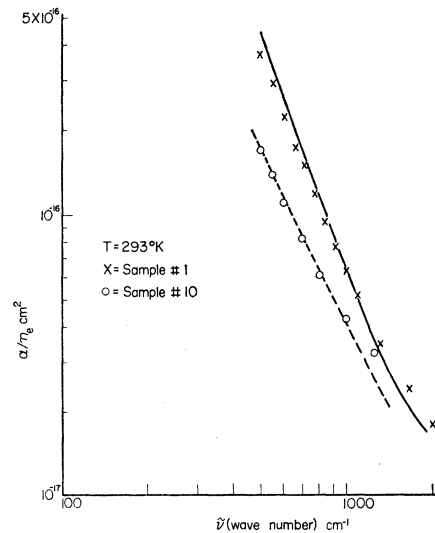

FIG. 1. Ratio of absorption coefficient to carrier concentration as a function of wave number.

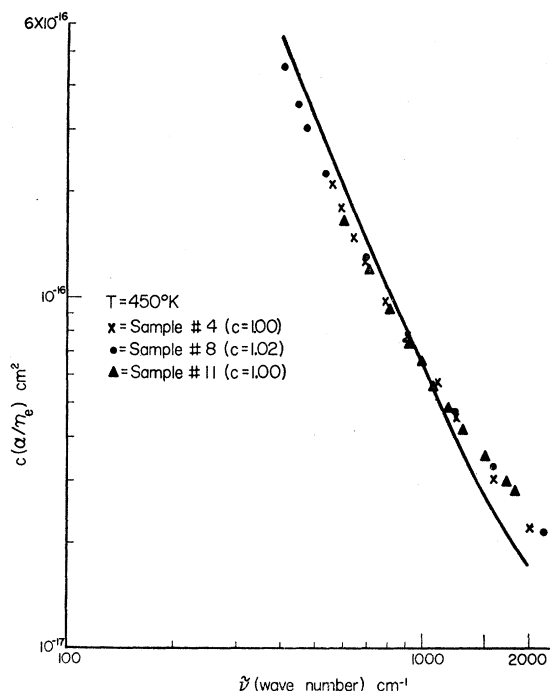[10] V. Johnson and K. Lark-Horovitz, Phys. Rev. **82**, 977 (1951).

FIG. 2. Ratio of absorption coefficient to carrier concentration as a function of wave number. The curve is calculated theoretically.

samples 1 to 5 are degenerate or nearly degenerate, and the Hall coefficient and resistivity of samples 6 to 12 give essentially the same values of n_e (within 10%) as obtained at room temperature. The values of impurity concentration, N_i, given in the last column were estimated from the impurity scattering mobility by using the Brooks-Herring formula.[11] The impurity scattering mobility was obtained from the carrier concentration, resistivity, and lattice scattering mobility.

In Fig. 1 are shown the results of the room temperature optical measurements on a pair of samples of different carrier concentrations. The ratio of the absorption coefficient to carrier concentration, α/n_e, is given as a function of wave number $\bar{\nu}$. Sample 1 appears to have a slightly steeper spectral dependence than does sample 10. This difference is characteristic of all samples measured; that is, samples of higher carrier concentration exhibit a steeper spectral dependence.

At 450°K, the spectral dependence is the same for all samples measured. This is illustrated in Fig. 2 where the measured points are shown for three samples of widely different carrier concentrations. The values of α/n_e for each sample have been multiplied by a constant, C, which is adjusted to bring the three samples to coincidence. The points from a common curve showing the absorption has the same frequency dependence in these samples, approximately propor-

[11] Discussed by P. P. Debye and E. M. Conwell, Phys. Rev. **93**, 693 (1954).

tional to $\bar{\nu}^{-2}$. This is true for all samples at this temperature. The values of the constant C are nearly the same for all three samples. The upper curve in Fig. 4 shows $\ln\alpha$ at $\bar{\nu}=1000$ cm^{-1} plotted against $\ln n_e$ for the different samples. The points lie closely to a straight line of slope 1 showing that α is proportional to n_e. In the case of samples 10 and 11, which have the smallest electron carrier concentrations, the absorption by holes is no longer negligible. In these two cases, it was necessary to subtract the absorption by holes from the total carrier absorption to obtain that due to the electrons. The hole absorption was determined from measurements of p-type germanium at the same temperature.

At 78°K, the dependence of α on $\bar{\nu}$ is again the same for all samples measured as indicated in Fig. 3. However, α increases more rapidly with λ than at the high temperature, approximately proportional to $\bar{\nu}^{-3}$. The values of the adjusting constant C indicate a lack of proportionality between α and n_e for different samples. The lower part of Fig. 4 shows the points of $\ln\alpha$ at $\bar{\nu}=1000$ cm^{-1} plotted against n_e for the different samples. A straight line of slope 1 cannot be drawn through these points. It will be noted that two points, those belonging to samples 6 and 12, have a much higher absorption than would be indicated by the rest of the samples. This pair of samples were doped with compensating impurities. The relatively high absorption of this pair of samples is an indication that the impurity content, as well as the carrier concentration, plays a role in determining the absorption.

From Figs. 1, 2, and 3, it is seen that absorption decreases with temperature. However, at sufficiently small wave numbers the absorption at 78°K becomes even larger than at room temperature (see Fig. 5). The wave number at which the absorption is equal for these temperatures decreases with decreasing N_i.
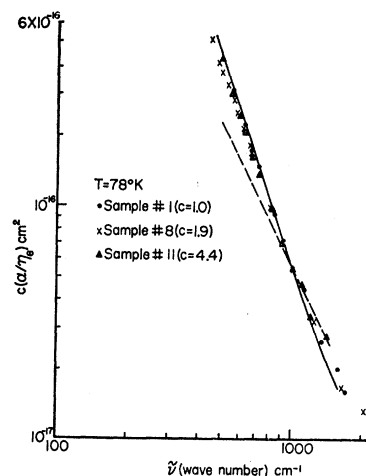

FIG. 3. Ratio of absorption coefficient to carrier concentration as a function of wave number. The solid curve is calculated for sample No. 1. The dashed curve is calculated for sample No. 11. [*Note:* In sample #8, "($C=1.9$)" should read "($C=2.5$)," and in sample #11, "($C=4.4$)" should read "($C=3.1$)."]
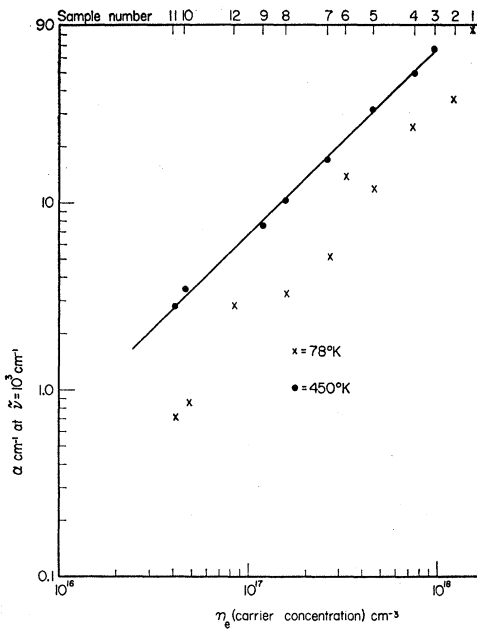
FIG. 4. Absorption coefficient at $\bar{\nu}=1000$ cm^{-1} for various samples as a function of carrier concentration.

DISCUSSION

The theoretical expressions (15) and (23) can be written as

$$\alpha/n_e = \left(\frac{m}{m^*}\right)^2 L(\bar{\nu},T) \quad \text{for lattice scattering,} \quad (25)$$

and

$$\alpha/n_e = N_i\left(\frac{m}{m^*}\right)^{\frac{3}{2}} I(\bar{\nu},T) \quad \text{for impurity scattering,}$$

where $L(\bar{\nu},T)$ and $I(\bar{\nu},T)$ are functions of temperature and wave number. The solid curves in Fig. 6 show $L(\bar{\nu},T)$ as a function of $\bar{\nu}$ for the three temperatures used in the absorption measurements. The factor σ_{l0}/τ^2 in (15) is equal to $n_e e^3/m^{*2}\mu_l$. The function L is calculated using $\mu_l = (4.9\times10^7/T^{1.66})$ cm^2 volt^{-1} sec^{-1}.[12] It is seen that the α/n_e for lattice scattering decreases and has a less steep spectral dependence as the temperature is decreased. The dashed curve in Fig. 6 is a similar graph for $I(\bar{\nu},T)$. The values calculated for 450°K and 78°K fall approximately on a common curve, showing the absorption to be insensitive to the temperature.

Due to the increasing absorption for lattice scattering with increasing temperature, this absorption mechanism should prevail at elevated temperatures. Indeed, the experimental results at 450°K are consistent with the expected behavior of absorption with lattice scattering, as indicated by the proportionality between α and n_e and the same frequency dependence shown by

[12] E. J. Morin, Phys. Rev. **93**, 62 (1954).

samples of different carrier concentrations. The curve in Fig. 2 is calculated using $m^*=0.10m$. It shows reasonable agreement with the experimental points.

At low temperatures, the α/n_e for imputiry scattering would be expected to be important because of the reduced absorption for lattice scattering. We would then expect α/n_e to vary among the samples depending upon the impurity concentration. The experimental results obtained at 78°K actually show such variation. Figure 7 is a graph of the experimental values of α/n_e at $\bar{\nu}=1000$ cm^{-1} as a function of N_i. The approximate relation indicated is

$$\alpha/n_e = A + BN_i = (0.17\times10^{-16} + 1.3\times10^{-35}N_i) \text{ cm}^2. \quad (27)$$

The term independent of N_i may be identified with the effect of lattice scattering while the term proportional to N_i should correspond to the effect of impurity scattering. The value of the constant term would be given by (25) if $m^*=0.11m$ is used, whereas the value of the coefficient of N_i would be given by (26) if $m^* = 0.083m_0$ is used. Using these values of A and B, curves can be calculated for all the samples. The solid curve in Fig. 3 is calculated for sample 1 of high impurity concentration and the dashed curve is calculated for sample 11 with small N_i. The curves are plotted using the same scale factors C as used in plotting the experimental points of the two samples. In sample 1, the effect of impurity scattering is large. The solid curve for this sample agrees very well with the experimental
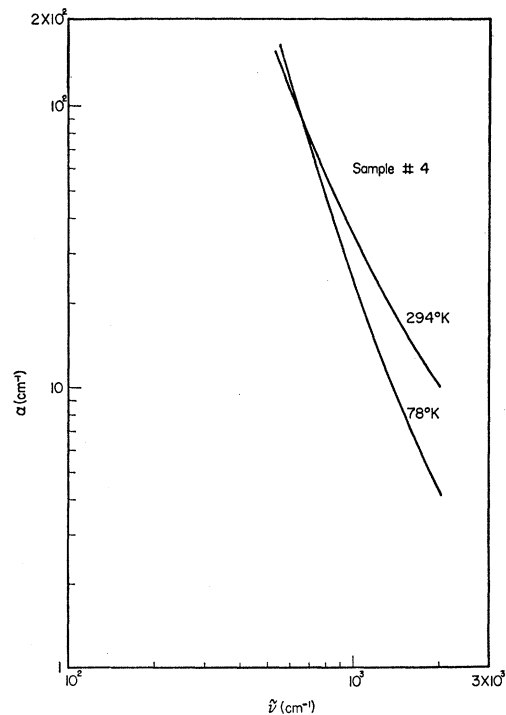

FIG. 5. Absorption coefficient as a function of wave number for a sample at two different temperatures.

points, indicating the correctness of $I(\bar{\nu})$ at this temperature. The dashed curve seems to be too flat, indicating that perhaps the theoretical formula for the effect of lattice scattering does not give sufficiently strong frequency dependence.

The best fit to the experimental results for room temperature is obtained by using $m^*=0.10m$ in both (25) and (26). Comparison between the calculated curves and the experimental points can be seen in Fig. 1 for two samples with high and low impurity concentrations. The agreement is good in both cases. The fact that at 78°K, the best fit is obtained with a somewhat lower value of m^* in (26) indicates that the theory may slightly underestimate the effect of impurity scattering at the low temperature. This interpretation is in line with the behavior shown in Fig. 5; according to the theory the absorption at the lower temperature should approach the absorption for the higher temperature but not exceed it.

On the whole, the theory is in reasonably good agreement with the observed absorption as a function of $\bar{\nu}$ and T for samples of different carrier and impurity

FIG. 7. Ratio of absorption coefficient to carrier concentration as a function impurity concentration.

concentrations. The effective mass needed to give the magnitude of absorption is about $0.1m_0$. This value is close to the conductivity effective mass, $0.12m$, according to the results of cyclotron resonance measurements made near the liquid helium temperature.[13] However, some microwave transmission measurements give larger values for the conductivity effective mass in the range of temperature covered by these absorption measurements.[14] The theoretical calculations are made assuming for simplification spherical surfaces of constant energy. For closer quantitative comparison with experiment, calculations should be made for the more complicated case of ellipsoidal surfaces of constant energy found in germanium.

There are eight minima or valleys at the bottom of the conduction band in germanium and electrons in each valley may be scattered into other valleys as well as into other states in the same valley. For the absorption with lattice scattering, the effect of intervalley scattering is roughly taken into account in (15) through the use of (13), since the relaxation time τ should include this effect. A more rigorous treatment requires information regarding the interaction $H^{(l)}$ for intervalley and intravalley scatterings. Although the expression (23) or (21) for the absorption with impurity scattering does not include the effect of intervalley scattering, the effect should be small due to the fact that $|\mathbf{k}_2-\mathbf{k}_1|$ is large in (17).
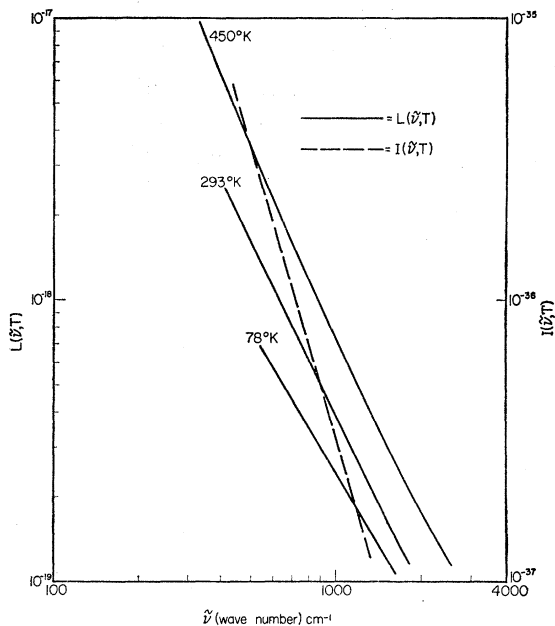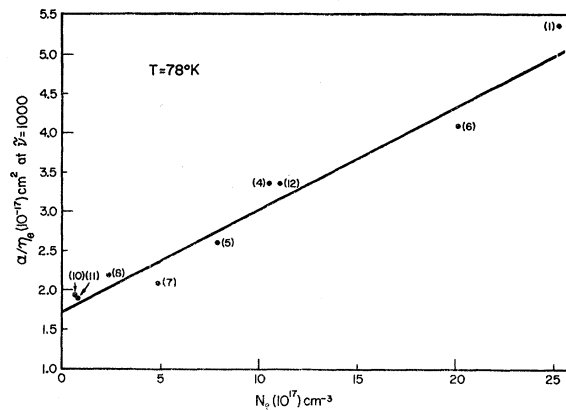

FIG. 6. The solid curves are theoretical functions $L(\bar{\nu},T)$ for absorption with lattice scattering plotted against $\bar{\nu}$ for three temperatures. The dashed curve gives the function $I(\bar{\nu},T)$ for absorption with impurity scattering; the curve applies for all three temperatures.

[13] Lax, Teiger, Dexter, and Rosenblum, Phys. Rev. **93**, 1418 (1954).

[14] T. S. Benedict and W. Shockley, Phys. Rev. **89**, 1152 (1953); F. D'Altroy and H. Y. Fan, Phys. Rev. **98**, 1561 (A) (1955).